

TiO₂ Coating for SnO₂:F Films Produced by Filtered Cathodic Arc Evaporation for Improved Resistance to H⁺ Radical Exposure

M.M. RISTOVA,^{1,5} A. GLIGOROVA,¹ I. NASOV,^{1,2} D. GRACIN,³ M. MILUN,⁴
H. KOSTADINOVA-BOSKOVA,² and R. POPESKI-DIMOVSKI¹

1.—Physics Department, Faculty of Natural Sciences and Mathematics, Gazi Baba bb, Skopje, R. Macedonia. 2.—Center for Plasma Technologies, PLASMA Ltd., Skopje, R. Macedonia. 3.—Institute Rudjer Boskovic, Bijenicka, Zagreb, Croatia. 4.—Institute of Physics, University in Zagreb, Bijenicka, Zagreb, Croatia. 5.—e-mail: mristova@pmf.ukim.mk

Titanium dioxide thin films were deposited by filtered cathodic arc evaporation (FCAE) from a Ti target in an oxygen atmosphere onto (a) fluorine-doped tin oxide substrates SnO₂:F (FTO) and (b) glass microscope slides. The growth rate calculated from film thickness profilometry measurements was found to be approximately 0.8 nm/s. The films were highly transparent to visible light. x-Ray photoemission spectroscopy analysis of the Ti 2p electron binding-energy shift confirmed the presence of a TiO₂ stoichiometric compound. The results for the root-mean-square (RMS) surface roughness of the films deposited onto FTO substrates evaluated by atomic force microscopy suggested nanostructured film surfaces. When exposed to hydrogen plasma, TiO₂ films revealed insignificant changes in the optical spectra. The initial sheet resistance of the SnO₂:F layer was 14 Ω/sq. The deposition of the top TiO₂ layer (45 nm thick) over the FTO electrode resulted in an increase of the sheet resistance of 2 Ω/sq. In addition, the sheet resistance of the double-layer FTO/TiO₂ transparent conductive oxide (TCO) electrode increased by 1 Ω/sq as a result of H⁺ plasma exposure. Regardless of the TiO₂ film's low conductivity, a thin protective layer could be coated onto FTO films (presumably 15 nm thick) due to their high transparency, offering high resistance to aggressive H⁺ plasma conditions. In this paper we show that ~50-nm-thick TiO₂ coating on FTO films provides sufficient protection against deterioration of transparency and conductivity due to hydrogen radical exposure.

Key words: TiO₂, thin-film coating, AFM, XPS, filtered cathodic arc evaporation (FCAE), transmittance, reflectance, H⁺ radicals, XPS, SEM, AXRD, XRR

INTRODUCTION

Titanium dioxide (TiO₂) is known as a wide-bandgap semiconductor with properties convenient for versatile industrial applications, such as for paints, ultraviolet (UV)-protection cosmetics, tooth-pastes, etc. In addition, it has been utilized for a wide range of high-technology applications, including

dye-sensitized solar cells,¹ photocatalysis,^{2,3} antireflective coating,⁴ gas sensing,⁵ and transparent heat mirrors.⁶ A recent publication by Kambe et al.⁷ showed that improvements of a-Si solar cell properties can be achieved by coating the SnO₂:F electrodes with an ultrathin TiO₂ layer. As reported by several groups of researchers, SnO₂:F (FTO) films coated with a thin layer of TiO₂ showed durability and high resistance to aggressive hydrogen plasma conditions.^{8,9}

TiO₂ films can be prepared by a variety of high- and low-cost technologies. Thin films for solar cell

(Received December 27, 2011; accepted August 2, 2012;
published online September 6, 2012)

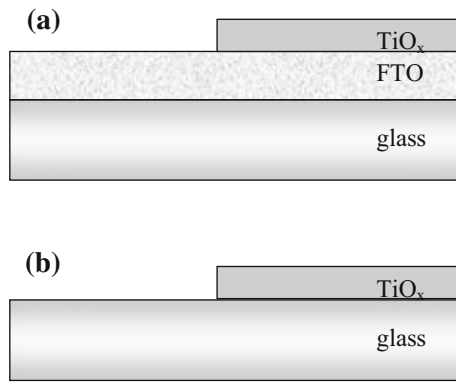


Fig. 1. Cross-section of TiO_2 prepared on (a) glass/FTO substrates and (b) glass substrates.

applications are usually produced by sol-gel techniques.¹ Other methods are also widely used, such as atmospheric-pressure chemical vapor deposition (APCVD),¹⁰ direct-current (DC) or radiofrequency (RF) sputtering,⁹ pulsed laser deposition (PLD),¹¹ filtered arc evaporation (FAE),¹² and solution growth.¹³

As was previously proven, applying an ultrathin TiO_2 coating to FTO films improves a-Si photovoltaic (PV) cell efficiency.⁷ TiO_2 coatings are of interest for their possible application in the a-Si PV industry; For instance, more in-depth research should be conducted on TiO_2 film's protective role against H^+ radical atmosphere. Furthermore, research showed that optical matching of the refractive indices in glass/FTO/ TiO_2 /Si multilayers required an optimal TiO_2 film thickness of 50 nm to 60 nm.⁹

The filtered cathodic arc evaporation (FCAE) method has been commonly used for deposition of a wide range of oxide and nitride films. This technique is known for its high ion energy (allowing high packing density of microparticles), high deposition rate, and flexibility of target arrangements. Using this technique, it is feasible to deposit TiO_2 amorphous films as high-quality optical coatings.¹⁴

In this work, we report on FTO coating with TiO_2 by the FCAE method from a Ti target in an oxygen atmosphere. The coatings were shown to be protective against FTO degradation in H^+ plasma conditions. The degradation effects due to H^+ radical exposure of TCO were studied by means of their optical and electrical changes. In addition, taking into consideration the results of this research and the requirements for optical matching of the refractive indices in glass/FTO/ TiO_2 /Si multilayers, we suggest that a sufficient thickness of TiO_2 coating to protect against FTO degradation in H^+ plasma should be approximately 50 nm.

EXPERIMENTAL PROCEDURES

Preparation and Growth Rate

Substrates (microscope glass slides and FTO precoated glass—product of Solar Split) were

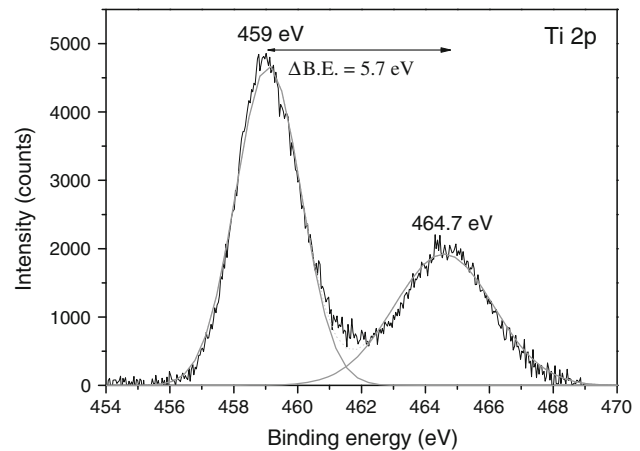


Fig. 2. XPS Ti 2p lines. The binding energy corresponds to TiO_2 stoichiometric compound.

degraded by acetone, then rinsed with deionized water, cleaned with isopropyl alcohol, and spun dry. The samples were then placed on a horizontal sample holder in a physical vapor deposition (PVD) chamber. A mixture of O/N plasma [total pressure 8 Pa, $V = 2$ kV, $I = 450$ mA (DC)] was applied for the 10-min ion beam cleaning procedure. The TiO_2 films were deposited by FCAE from a Ti target of 99.9% purity in an O_2 atmosphere. Upon reaching the deposition vacuum of 2×10^{-2} Pa, the partial pressure of oxygen was adjusted to 3.5 kPa. Prior to the deposition procedure, half of the area of each substrate was covered by a glass microscope slide to prevent TiO_2 deposition. The substrates were then placed into an industrial-scale FCAE deposition system (product of Ukrainian Academy of Science Vacuum Systems), designed for use in coating industries. The system incorporated a filter which effectively removes microparticles. A Ti cylinder (55 mm diameter, 1730 mm height) was used as a target. The substrates were not intentionally heated. However, substrate heating resulted from heat transfer during the sublimation of the evaporated material as well as from conversion of kinetic energy from the particles hitting the target into heat. The titanium cathode was operated at arc current of 120 A. The voltage of the target switched between 30 V and 80 V. The distance between the Ti cathode and the substrates was 170 mm. The flow rate of O_2 was set to 30 sccm, yielding process pressure of 1.2 Pa. The aforementioned procedure allowed deposition of TiO_2 samples with different film thicknesses depending on the deposition time (from 0.5 min to 15 min). Cross-sections of the prepared model samples (TiO_2 /FTO/glass and TiO_2 /glass), used for different research purposes, are depicted in Fig. 1. For the prescribed conditions (voltage, current, and pressure), the growth rate was established on the dependence of the TiO_2 film thickness on the deposition time. The TiO_2 film thickness of the various samples was derived from

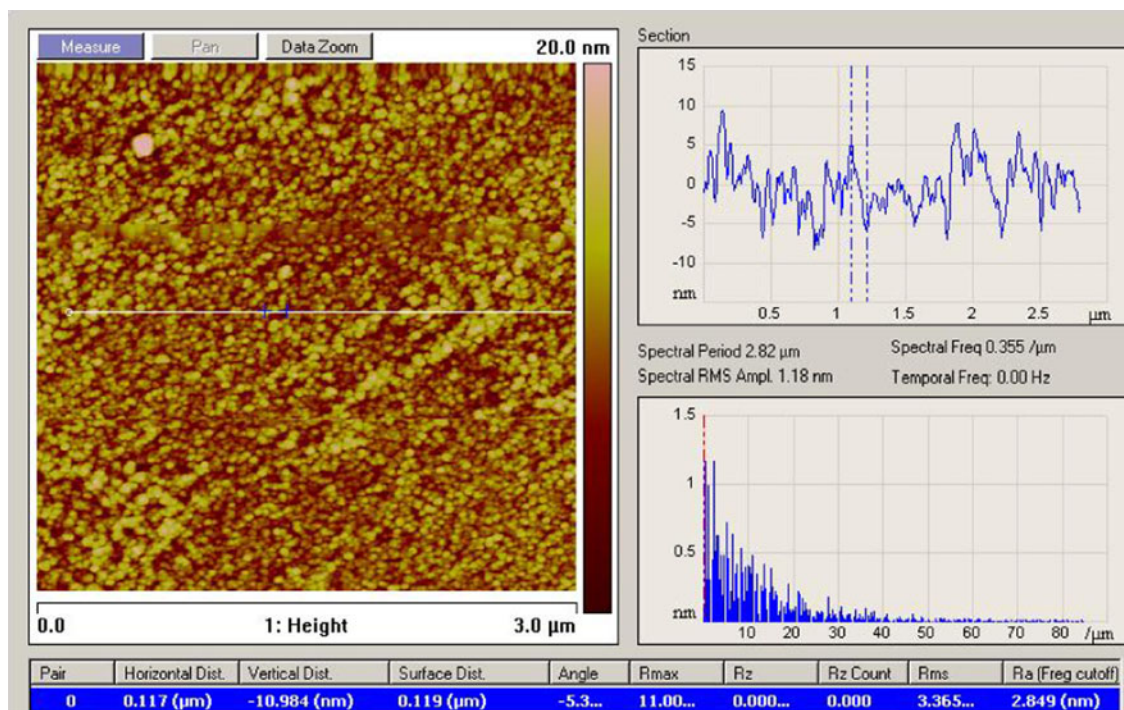


Fig. 3. AFM from a TiO₂ film surface deposited by FCAE on a microscope glass substrate for 15 min (estimated thickness of about 675 nm). The calculated RMS of the surface is 3 nm.

various types of measurements: profilometry measurements with a Tencor Alfa Step profilometer on the TiO₂ step, scanning electron microscopy (SEM) on the film cross-section, and specular x-ray reflection (XRR).

Surface Analysis

The TiO₂ film thickness depended on the deposition time.

x-Ray photoelectron spectroscopy (XPS) using Al K_α radiation was employed for qualitative analysis of the TiO₂ compound produced by the described PVD-FCAE deposition method. The Ti 2p electron line doublet was subjected to electron energy shift analysis. The XPS instrument consisted of a monochromatized x-ray source with a Mg–Al dual anode and a hemispherical electrostatic electron analyzer (VSW HA100) under the following operation conditions: fixed analyzer transition (FAT) mode at 50 eV with resolution of 1.1 eV. The Ti 2p electron binding-energy doublet line was subjected to qualitative analysis.

Asymmetric x-ray diffraction (AXRD) measurements are suitable for surface characterization and thin-film structure analysis. Specular x-ray reflectivity (XRR) measurements were conducted using a conventional laboratory small-angle x-ray scattering (SAXS) experimental setup, modified and adapted with a tilting specimen stage for grazing incidence, using Cu radiation ($\lambda = 0.154$ nm). The diffracted x-rays were collected with a curved sensitive detector (RADICON), allowing simultaneous

recording of the XRD pattern within the 2θ range from 20° to 65°. The asymmetrical geometry under fixed grazing incidence angle α_i ($\alpha_i > \alpha_C$) amplified radiation originating mainly from the surface layer. α_C is the critical angle for total external reflection. The reflectivity spectra were captured with a sensitive detector (M.BRAUN PSD-50M), positioned in the specular plane. An attenuator was used for angles lower than the predefined angle to avoid damage to or saturation of the detector by the intense reflected radiation. The attenuation factor was automatically computed during the measurements, enabling a dynamical scale of several orders of magnitude.

Atomic force microscopy (AFM) scans were made by using a Nanoscope III AFM from Veeco. Calculations of the film's surface roughness were carried out for the RMS of the different samples. Two-dimensional (2D) AFM presentations and the calculations of the RMS roughness were carried out using the WSxM-Image Browser software tool.

Hydrogen Radical Exposure of the TiO₂-Coated TCO

A pulsed glowing discharge chamber (50 kW ION-50 I, product of Ukrainian Academy of Science Vacuum Systems) with working dimensions ϕ 1000 × 1000 mm was employed for investigation of the impact of hydrogen radicals on both the TiO₂-coated and bare FTO thin film. The chamber was originally designed for industrial plasma nitrating. Upon application of 0.6 kV, a hydrogen plasma was

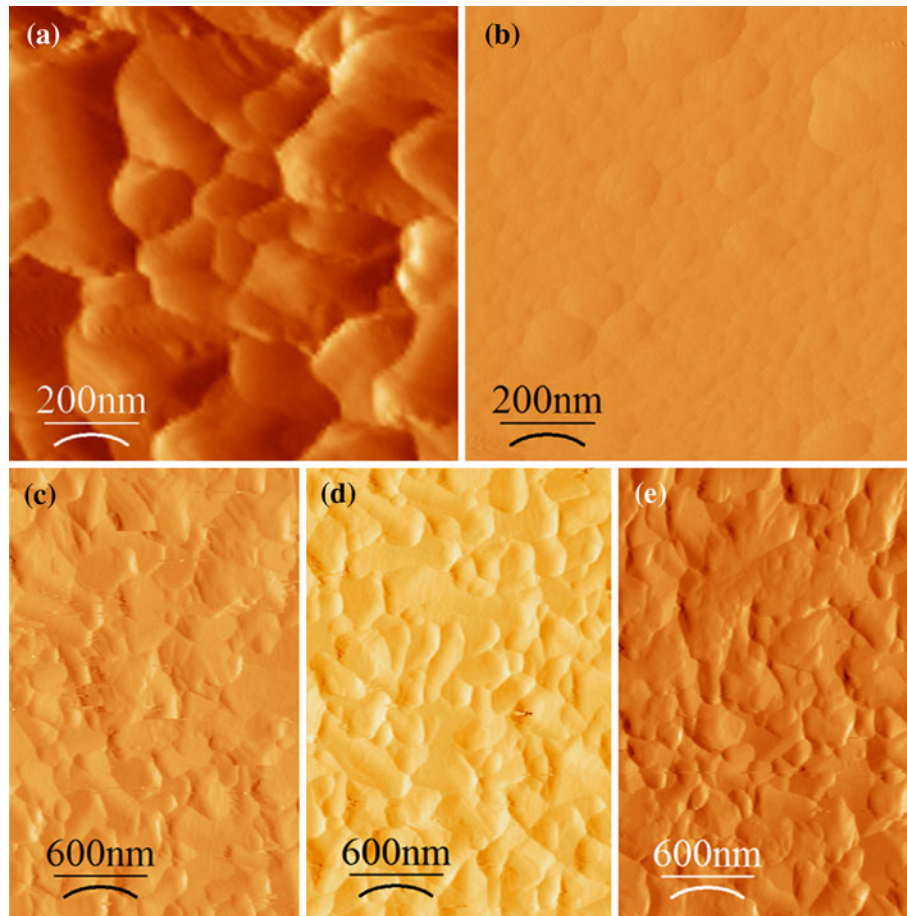


Fig. 4. 3D-effect AFM presentations of the following surfaces: (a) glass/FTO (RMS = 54 nm), (b) glass/TiO₂ (RMS = 5 nm), (c) glass/FTO/TiO₂ film (30 s—RMS = 39.8 nm), (d) glass/FTO/TiO₂ (1 min—RMS = 36.9 nm), and (e) glass/FTO/TiO₂ (5 min—RMS = 26.5 nm).

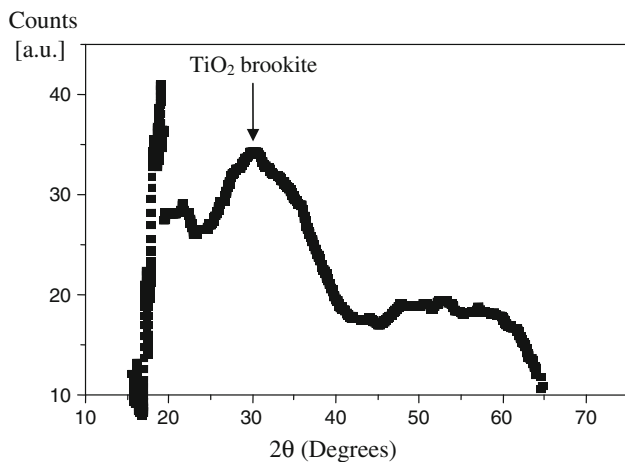


Fig. 5. AXRD pattern of TiO₂ coating on FTO, deposited for 30 s.

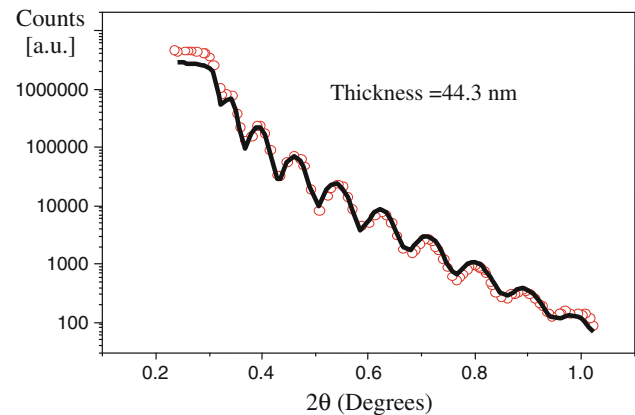


Fig. 6. XRR graph of the TiO₂ film (deposition time 30 s).

generated between the anodic furnace wall and the cathodic disk, producing active hydrogen radicals for film exposure. The H⁺ plasma thermal conditions were as follows: from room temperature to 120°C, the sample temperature increased at a rate of 10°C/min. Before the heating, the chamber

pressure was 70 Pa. The H₂ partial pressure in the chamber during heating of the sample to 120°C (14 min) decreased from 300 Pa to 100 Pa. The sample was exposed to pure H⁺ plasma at H₂ partial pressure of 100 Pa for 10 min. Hence, the total exposure time of the sample to H⁺ plasma

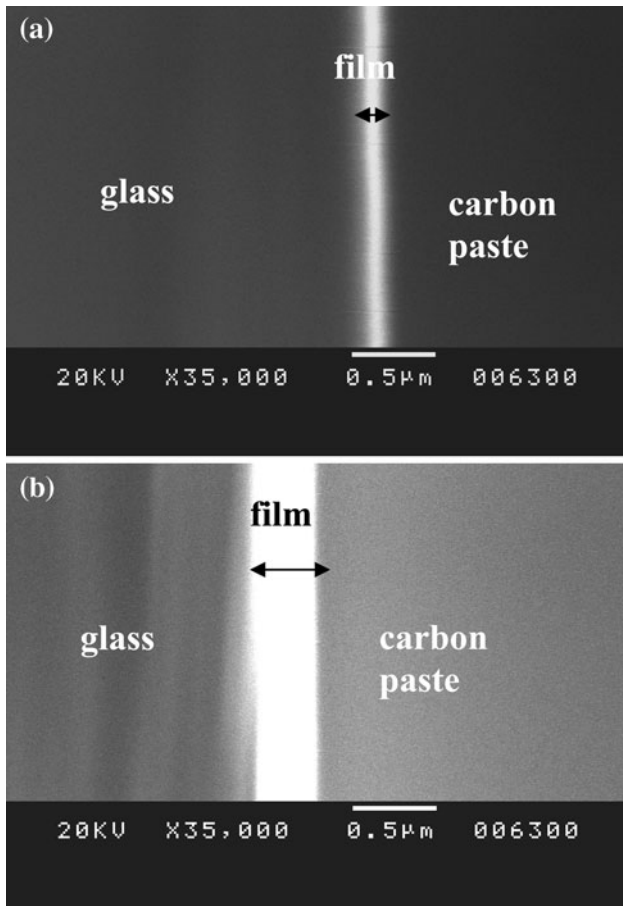


Fig. 7. SEM of the cross-section of the interface glass/TiO₂/carbon paste. (a) TiO₂ deposited for 1 min (film thickness ~100 nm) and (b) TiO₂ deposited for 9 min (film thickness ~400 nm).

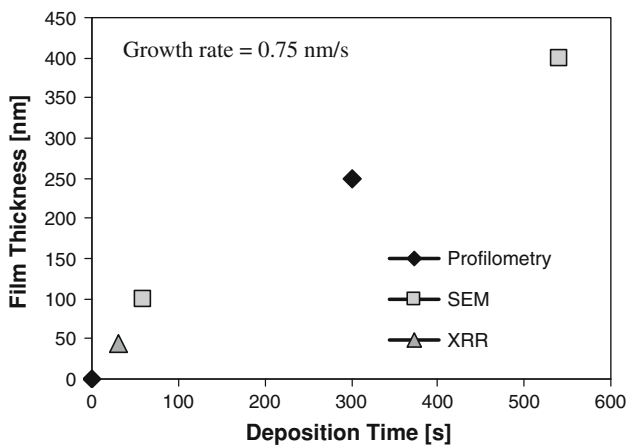


Fig. 8. Variation of film thickness with deposition time. The growth rate of TiO₂ film deposited by FCAE was derived by linear fitting.

was 24 min. The average current density was 0.6 mA/cm².

The influence of the H⁺ plasma on the TiO₂-coated and uncoated TCO samples, depicted in Fig. 1, was studied with the following procedure:

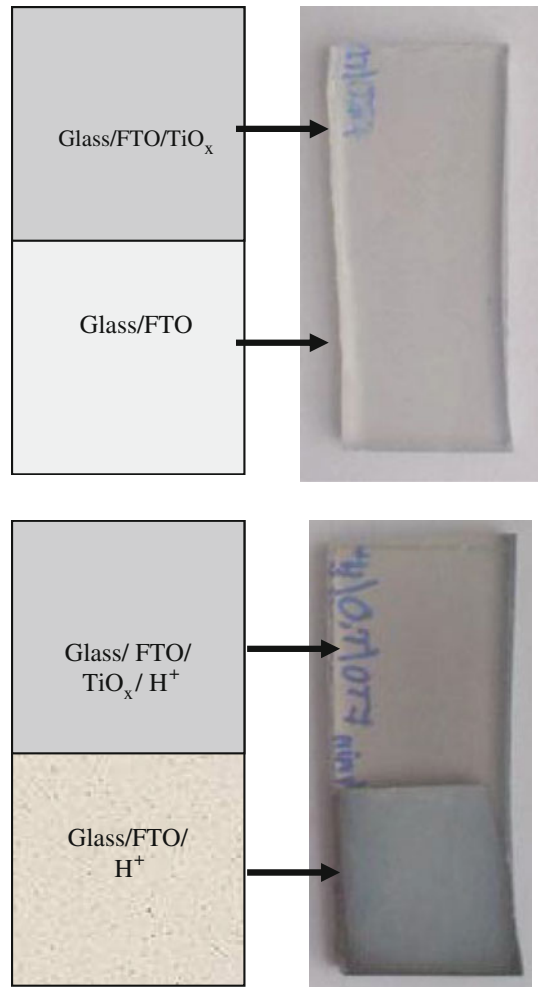


Fig. 9. Photographs against a white paper background in daylight of the following samples: glass/FTO, glass/FTO/TiO₂, glass/FTO/H⁺, and glass/FTO/TiO₂/H⁺, showing the influence of H⁺ plasma on film transparency in white light.

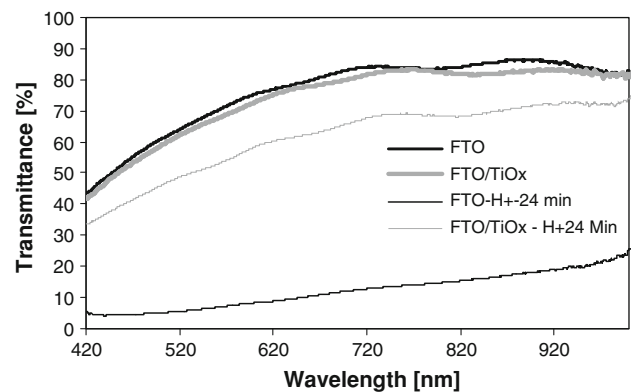


Fig. 10. VIS-NIR transmittance spectra of both uncoated and TiO₂-coated FTO films, before and after H⁺ plasma exposure.

- (a) Two identical FTO samples were prepared for coating;
- (b) TiO₂ film (approximately 45 nm) was deposited on half of the area of each of the FTO films (one

- half was kept covered during the TiO₂ deposition);
- (c) One of the two prepared identical films (half of the area of the glass/FTO coated with TiO₂) was exposed to H⁺ plasma for 24 min under heavy H⁺ radical conditions [4 to 5 times longer exposure at conditions similar to those used in industrial a-Si plasma-enhanced chemical vapor deposition (PECVD) processes]; The other sample from (b) was kept unexposed to H⁺ radicals to be used later for comparison;
- (d) Finally, the influence of the H⁺ plasma on the TCO surface was studied on the following four areas of the two samples: glass/FTO, glass/FTO/TiO₂, glass/FTO/H⁺, and glass/FTO/TiO₂/H⁺ (as depicted in Fig. 9).

Optical Spectra and Conductivity

The film's optical transparency was examined by visible and near-infrared (VIS-NIR) spectroscopy, using an Ocean Optics HR4000 spectrophotometer and a white light source. Likewise, the reflectance spectra were examined with an additional optical reflection setup with a Mikropack ISP-80-8-REFL integrating sphere with internal diameter of 80 mm and sample port diameter of 8 mm. The IR transmittance spectra were also taken from all four sample areas, as depicted in Fig. 9.

The TCO sheet resistance of each of the four samples (uncoated and TiO₂-coated FTO, before and after H⁺ exposure) was measured with an ohmmeter using a two-electrode setup, with two parallel silver paste electrodes painted across the sample's surface (2.5 cm long, 2.5 cm apart). The impact of the H⁺ radicals on both the film sheet resistance and the optical spectra (VIS/IR) was studied and is discussed below.

RESULTS AND DISCUSSION

Surface Analysis of TiO₂ Films (XPS, AXRD, XRR, and AFM)

XPS spectra were taken from the TiO₂ as deposited onto the FTO precoated glass. Initially, a broad XPS spectrum was taken. The C 1s line was fixed at 285 eV. The typical Ti 2p_{1/2} and Ti 2p_{3/2} lines were selected for qualitative analysis. The Ti 2p peak doublet was Gauss-fitted, and the binding-energy maxima were obtained at 464.7 eV and 459 eV (Fig. 2). The position of the main peak Ti 2p_{3/2} (Fig. 2) appeared at 459 eV, which is very close to the Ti 2p_{3/2} electron binding energy reported for Ti 2p electrons for the Ti⁴⁺ oxidation state.¹⁵ Other authors report that the Ti 2p_{3/2} peak for the TiO₂ stoichiometric compound appears at 458.5 eV.¹⁶ Moreover, the binding-energy difference for the examined Ti 2p electrons was found to be ΔBE = 5.7 eV, which could be strongly attributed to

the TiO₂ compound.^{15,16} Hence, the XPS qualitative analysis showed that the described FCAE grows stoichiometric TiO₂ films.

An AFM scan from a TiO₂ film surface deposited by FCAE on a microscope glass slide for 15 min (estimated thickness of 675 nm) is shown in Fig. 3. The obtained RMS surface roughness was about 3 nm. In a similar manner, three-dimensional (3D) AFM surface images were obtained for the following surfaces: (a) glass/FTO (Solar-Split), (b) glass/TiO₂ (15 min deposition time), (c) glass/FTO/TiO₂ film (30 s), (d) glass/FTO/TiO₂ (1 min), and (e) glass/FTO/TiO₂ (5 min), as presented in Fig. 4. The results for the RMS surface roughness of the films deposited onto FTO substrates suggested nanostructured surfaces of the TiO₂ compound. As can be observed in Fig. 4a, b, the surface of the uncoated FTO/glass sample is approximately 20 times rougher than the surface of the TiO₂/glass coating itself (56 nm and 3 nm, correspondingly). As can be observed, the TiO₂ coating on the rough FTO layer facilitates smoothening of the overall TCO surface. As a result, with the TiO₂ coating, the RMS of the FTO decreased from 56 nm for the bare FTO to 39.8 nm for the 30 s coated and to 26.5 nm for the 300 s coated TCO.

AXR diffraction was recorded at grazing incidence angle at 0.35°, which was sufficiently large to facilitate penetration of the x-rays through the sample's surface but sufficiently small to induce scattering mainly from the surface layer ($\alpha_C = 0.28^\circ$). In Fig. 5 the net AXRD pattern is plotted after normalization and subtraction of the background substrate intensity. For this purpose, AXRD data of the substrate (microscope glass) were collected under the exact same experimental conditions. As can be seen in Fig. 5, the net signal was weak and contained broad maxima centered at 2θ angles of about 30° and 54°. The maximum at 30° could be associated to a disordered/amorphous brookite-like TiO₂ structure, which according to the literature shows strong Bragg reflections at 29.4°, 29.8°, and 35.7°.^{17,18}

The specular XRR data of the TiO₂ sample deposited during 30 s are presented on a log-linear plot of intensity versus incidence angle in Fig. 6. From the full fit of the reflectivity curve (full line) it was calculated that the film thickness was 44.3 nm and the α_C /density of the top layer was 0.28°/3.74 g/cm³. Furthermore, the surface roughness of the TiO₂ and the roughness at the TiO₂/glass interface were calculated to be about 1.5 nm, which appeared to be half of the value obtained from the AFM scans. The density of the top layer was found to correspond to the nominal value of brookite (4.07 g/cm³) within the experimental error, which represents 96% of the densely packed rutile crystalline phase. For comparison, the density of titanium element is 4.50 g/cm³ and the densities of some other TiO₂ phases are as follows: rutile—4.25 g/cm³, anatase—3.89 g/cm³.

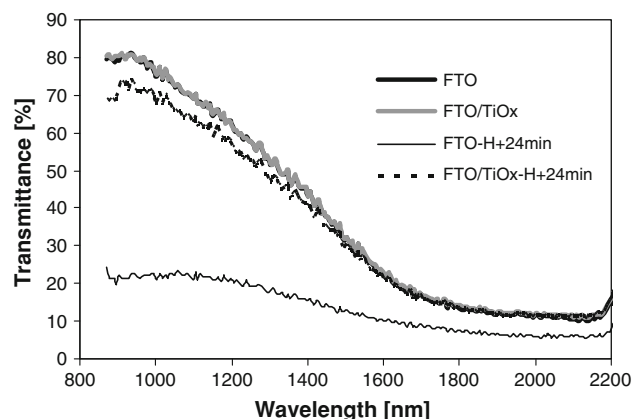


Fig. 11. IR transmittance spectra of both uncoated and TiO₂-coated FTO films, before and after H⁺ plasma exposure.

Growth Rate of TiO₂ Films

The thickness of the TiO₂ film deposited for 30 s was obtained from the reflectivity (XRR) graph. The thicknesses of the TiO₂ films deposited during 1 min and 9 min were obtained from SEM scans of the film cross-sections (Fig. 7a, b). The thicknesses of the films deposited for 5 min and 15 min were obtained from profilometry measurements. The growth rate of the TiO₂ films grown by FCAE was established from the slope of the graphical presentation of film thickness versus deposition time (Fig. 8). The growth rate line was fixed to zero thickness for the start time. Hence, it can be established that, under the prescribed deposition conditions, the TiO₂ growth rate is 0.75 nm/s (2.7 μm/h). Similar growth rates have been reported by other authors for TiO₂ film deposition by arc evaporation (0.5 nm/s).¹² These results show that the FCAE method facilitates much faster TiO₂ film growth compared with RF sputtering. The considerable growth rate, superior to both DC and RF sputtering,⁹ makes this method convenient for time-efficient industrial-scale PV production.

Influence of H⁺ Radicals on the Optical Properties and Sheet Resistance of TCO

Daylight photographs of the films, subject to optical and conductivity examinations, are shown in Fig. 9. Figures 10, 11, and 12 show the VIS-NIR transmittance, IR transmittance, and VIS reflectance spectra of the corresponding films. The presented VIS and IR transmittance spectra (Figs. 10 and 11) clearly reveal that the 45-nm TiO₂ coating on FTO protects against transparency decrease during H⁺ radical exposure. Both the VIS and IR transmittance spectra also show that application of the TiO₂ coating over the FTO invoked insignificant changes in the transparency. However, the figures

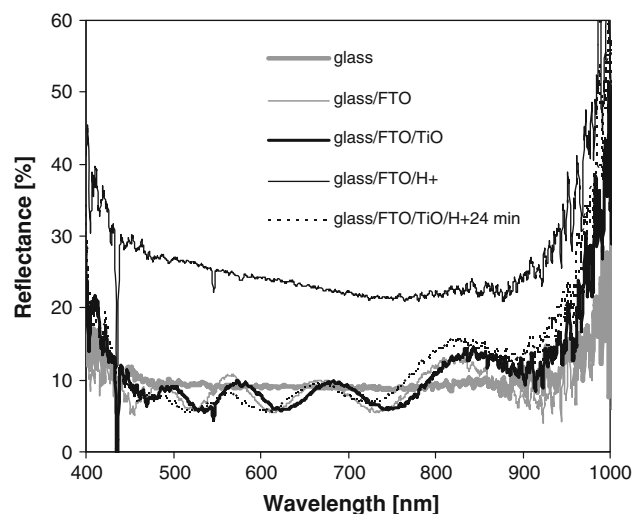


Fig. 12. VIS-NIR reflectance spectra of both uncoated and TiO₂-coated FTO films, before and after H⁺ plasma exposure.

show that the transmittance of the bare FTO films is substantially degraded as a consequence of H⁺ exposure (by over 50%). The same graphs reveal minor transparency changes (about 10%) of the TiO₂-coated FTO as a result of H⁺ exposure. Figure 12 shows that the spectral reflectance of the uncoated FTO sample increased from 10% to about 30% as a result of H⁺ exposure, whilst the reflectance of the TiO₂-coated FTO sample changed inconsiderably. Moreover, according to Fig. 12, the reflectance interference pattern shows changes that suggest a change of either refractive index (n) or film thickness (d). It could be speculated that it seems far less probable that penetration of protons (H⁺) induces an etching effect (thickness change) of the TiO₂ film, since TiO₂ films are a well-known H⁺ barrier. However, it seems more likely that incorporation of H⁺ radicals will induce compositional changes, resulting in variation of the refractive index. The latter remains to be studied in the future. Hence, application of the TiO₂ coating on FTO also prevents deterioration of the film reflectance, which appears to be an undesired consequence of H⁺ exposure.

The second crucial parameter of TCO for PV applications, the sheet resistance, was studied by means of its variation due to FTO coating with TiO₂, before and after H⁺ radical exposure. It is evident from the results presented in Table I that the sheet resistance of the bare (as produced by the factory) FTO substrate (~400 nm thick) was 14 Ω/sq, and that deposition of a 45-nm TiO₂ protective coating increased the sheet resistance to 16 Ω/sq (increase by 2 Ω/sq). Finally, as a result of H⁺ radical exposure, it is evident that the sheet resistance increased from 14 Ω/sq to 26 Ω/sq for the uncoated FTO, while for the TiO₂-coated FTO it increased from 16 Ω/sq to 17 Ω/sq.

Table I. TCO sheet resistance of both uncoated and 45-nm TiO₂-coated FTO, before and after H⁺ exposure

Film	Sheet Resistance (Ω/sq)
FTO	14
FTO/TiO ₂	16
FTO/H ⁺	26
FTO/TiO ₂ /H ⁺	17

CONCLUSIONS

The FCAE method provides fast growth (0.75 nm/s) of highly transparent TiO₂ films. The method provides much faster growth than RF sputtering, making FCAE more economical for industrial-scale a-Si PV production.

The FCAE method under the described conditions produced stoichiometric TiO₂ films with disordered/amorphous brookite-like structure with surface roughness of about 3 nm, as calculated from AFM scans, or about 1.5 nm, as calculated from the XRR pattern. This discrepancy probably results from the influence of the area scanned in the AFM measurements on the calculated RMS values. FTO films coated with TiO₂ appeared to be resistant to extreme H⁺ radical conditions, as their transparency and reflectance changed insignificantly. A 45-nm TiO₂ protective coating on the FTO increased the TCO's initial sheet resistance by 2 Ω/sq . The protective TiO₂ coating resulted in inconsiderable overall degradation of the TCO properties on H⁺ radical exposure. Considering the respectable transparency and antireflective properties of the a-Si/FTO sandwich, the smoothness (RMS = 3 nm), as well as their high resistance to extreme H⁺ radical conditions, one could conclude that FCAE-deposited TiO₂ films of about 50 nm thickness could be incorporated into a-Si PV cell technology to increase the cell efficiency. Moreover, ~50-nm-thick coatings seem to be appropriate also in terms of refractive index matching of the multilayers, since the optimum thickness, as calculated by other

authors, was found to be approximately 50 nm.⁹ However, reduction of the TiO₂ film's resistivity should be sought in the future; doping with nitrogen could be considered as a promising method.⁹

ACKNOWLEDGEMENTS

We would like to gratefully acknowledge the financial support of the European Commission (Project LPAMS 2004–2007 from the FP-6 INCO Program) and the technical support by Plasma Technologies-Skopje in facilitating the FCAE deposition and H⁺ radical exposure in 2007.

REFERENCES

1. B. O'Regan and M. Grätzel, *Nature* 353, 737–740 (1991).
2. A. Fujishima and K. Honda, *Nature* 238, 37 (1972).
3. M.R. Hoffmann, S.T. Martin, W. Choi, and D.W. Bahnemann, *Chem. Rev.* 95, 69 (1995).
4. C. Martinet, V. Pillard, A. Gagnaire, and J. Joseph, *Non-Cryst. Solids* 216, 77 (1997).
5. D. Manno, G. Ricoci, R. Rella, A. Serra, A. Taurino, and A. Tepore, *J. Appl. Phys.* 82, 54 (1997).
6. C.G. Granqvist, *Materials Science for Solar Energy Conversion Systems* (Oxford: Pergamon, 1991).
7. M. Kambe, M. Fukawa, N. Taneda, and K. Sato, *Sol. Energy Mater. Sol. Cells* 90, 3014 (2006).
8. H. Natsuhara, T. Ohashi, S. Ogawa, N. Yoshida, T. Itoh, S. Nonomura, M. Fukawa, and K. Sato, *Thin Solid Films* 430, 253 (2003).
9. H. Natsuhara, K. Matsumoto, N. Yoshida, T. Itoh, S. Nonomura, M. Fukawa, and K. Sato, *Sol. Energy Mater. Sol. Cells* 9, 2867 (2006).
10. K. Sato, Y. Gotoh, Y. Hayashi, K. Adachi, and H. Nishimura, *Reports Res. Lab. Asahi Glass Co. Ltd.* 40, 233 (1990).
11. A. Buzas, L. Egerhazi, and Zs. Geretovszky, *J. Phys. D Appl. Phys.* 4, 085205 (2008).
12. P.J. Martin, R.T. Netterfield, and T.J. Kinder, *Thin Solid Films* 193, 77 (1990).
13. S. Deki, Y. Aoi, O. Hiroi, and A. Kajinami, *Chem. Lett.* 6, 433 (1996).
14. Z. Zhao, B.K. Tay, and G. Yu, *Appl. Opt.* 4, 1281 (2004).
15. XPS, *Handbook of Elements and Native Oxides* (XPS International Inc., Mountain View, 1999).
16. G.E. Muilenberg, eds., *Handbook of X-Ray Photoelectron Spectroscopy* (Boston: PerkinElmer Corporation, 1979).
17. IEM Databases and Datasets, Russian Foundation of Basic Research, <http://database.iem.ac.ru/mincryst/mixipol.php?brook.it1+2>. Accessed 21 August 2012.
18. S.R. Yoganarasimhan and C.N.R. Rao, *Anal. Chem.* 33, 155 (1960).